

Robustness of kinematic weighting and scaling concepts for musculoskeletal simulation

Florian Schellenberg, William R. Taylor, Ilse Jonkers & Silvio Lorenzetti

To cite this article: Florian Schellenberg, William R. Taylor, Ilse Jonkers & Silvio Lorenzetti (2017) Robustness of kinematic weighting and scaling concepts for musculoskeletal simulation, Computer Methods in Biomechanics and Biomedical Engineering, 20:7, 720-729, DOI: [10.1080/10255842.2017.1295305](https://doi.org/10.1080/10255842.2017.1295305)

To link to this article: <https://doi.org/10.1080/10255842.2017.1295305>



© 2017 The Author(s). Published by Informa UK Limited, trading as Taylor & Francis Group



Published online: 01 Mar 2017.



Submit your article to this journal [↗](#)



Article views: 1385



View related articles [↗](#)



View Crossmark data [↗](#)



Citing articles: 4 View citing articles [↗](#)

Robustness of kinematic weighting and scaling concepts for musculoskeletal simulation

Florian Schellenberg^a, William R. Taylor^a, Ilse Jonkers^b and Silvio Lorenzetti^a

^aInstitute for Biomechanics, ETH Zurich, Zürich, Switzerland; ^bDepartment of Kinesiology, Katholieke Universiteit Leuven, Leuven, Belgium

ABSTRACT

Musculoskeletal modelling is widely used to estimate internal loading conditions. In order to optimise robustness and reduce errors between the subject-specific reference motion data (RMD) and the musculoskeletal simulation, 90 permutations of kinetic and kinematic data were analysed during split squats. A ranking for the scaling and kinematic weighting concepts based on the RMS errors when including functional centres of rotation (*fCoRs*), joint angles, and skin markers, revealed that analyses should include *fCoR* in the scaling and the simulation processes, as well as an automated weighting procedure including all attached skin markers for optimal registration of the musculoskeletal model to the RMD.

ARTICLE HISTORY

Received 3 May 2016
Accepted 11 February 2017

KEYWORDS

Subject specific
musculoskeletal modelling;
robustness; error estimation;
strength training; split squats


Introduction

Musculoskeletal (MS) simulation plays a key role in biomechanics for estimating internal loading conditions, including muscle and joint contact forces. More specifically, knowledge of the internal forces has been extensively used to provide improved understanding of clinical treatments e.g. joint replacement (Delp et al. 1990; Piazza & Delp 2001) and its outcome (Jonkers et al. 2008), or muscle replacement in crouch gait children (Delp et al. 2007), but also to estimate the loading conditions in sports and activities of daily living (Pandy et al. 1990; van Soest et al. 1993; Bobbert 2001; Liu et al. 2006; Lewis et al. 2009; Blajer et al. 2010). Direct measurement of muscle and joint contact forces is currently not possible, resulting in the recent development of MS modelling techniques that are able to provide access to these parameters, albeit indirectly, by means of numerical optimisation processes (Schellenberg et al. 2015). As a result of the detailed modelling approaches required to accurately determine the kinetics of the human body, MS simulation software packages such as Anybody (Anybody Technology, Aalborg, Denmark), OpenSim (Simtk, Stanford, CA, United States; Delp et al. 2007), Biomechanics of Body (BoB; Shippen & May 2010) and others have become widely available.

A common approach for generating MS simulations is to first scale a reference MS model that possesses generic

anthropometrical parameters, such as height, body weight, segment lengths, muscle paths etc. to the specific subject in question. The second step is to calculate the body/segment kinematics from e.g. skin marker trajectories or joint angles captured during the target movement. Finally, the scaled model and the calculated segment kinematics are combined with measured kinetic data to allow estimation of the internal loading conditions by means of inverse dynamics and optimisation processes to solve the muscle distribution problem (Schellenberg et al. 2015).

The accurate measurement of segment kinematics is challenging due to the complexity of the soft tissues moving relative to the underlying skeletal structures (Taylor et al. 2005; Zemp et al. 2014). As a result, motion capture varies from techniques using data extracted from simple videos, through retro-reflective markers attached to the subject's skin, to extensive measurement using e.g. video-fluoroscopy (Banks & Hodge 1996; List, Foresti, et al. 2012; List, Gerber, et al. 2012), MRI (Arnold et al. 2010) or ultrasound (Ito et al. 2000). However, due to their increasing availability, non-invasive, high-speed and accurate nature, optoelectronic infra-red measurement devices have now become a standard technique for the capture of human movement. In order to improve the robustness of MS simulations (De Groote et al. 2010; Lu et al. 1997), specific approaches for the reduction of soft tissue artefact (Taylor et al. 2005) and the assessment of the underlying

CONTACT Silvio Lorenzetti  sl@ethz.ch

skeletal kinematics (Charlton et al. 2004; Ehrig et al. 2006, 2007; Taylor et al. 2010) have been developed (Peters et al. 2010) and are now even integrated within commercial motion capture software (e.g. Vicon).

In order to understand the subject specific loading conditions based on the measured kinematic data, approaches to register reference MS models to the individual's anatomy and kinematics are required. However, the accuracy of a simulation is known to be sensitive to the subject specific anatomical specification, including bone and muscle architecture (Arnold et al. 2010). Therefore, the scaling processes, as well as the method of including kinematic data into the simulation, will influence the resulting internal loading conditions in a complex manner (Correa & Pandy 2011; Winby et al. 2008). With the aim of enhancing the physiological validity and accuracy of the segment kinematics, different methodologies for weighting the motion capture data (Heller et al. 2011) and/or geometrical parameters, such as human shape, bone structure or muscle paths, are also thought to improve the robustness of MS models (Moeslund et al. 2006). Consequently, reconstruction of a subject's original motion and kinetics, using specific scaled MS models involves many unknowns and assumptions, making the result highly sensitive to the considerable number of settings used during the scaling and kinematics registration.

With numerous approaches for scaling and fitting model anatomic and kinematic data, it is often unclear how the settings used during scaling and kinematics registration can best be utilised to allow the motion patterns that were actually measured to be reconstructed in the MS model. Therefore, the aim of this study was to quantify the

robustness of MS simulation in OpenSim using different scaling methods and differently weighted kinematic concepts, as well as to estimate the resulting errors in terms of kinematics and kinetics.

Methods

Kinematic and kinetic data

The data used in this study was captured previously in 11 subjects for the analysis of loading conditions in the lower limbs during six repetitions of 10 different types of split squats, leading to 660 cycles (Schütz et al. 2014). Split squats are a common multi-joint strength exercise to train mainly the *m. gluteus maximus*, *m. iliopsoas*, quadriceps, and hamstrings (Graham 2002) in a slow, non-impact manner. Their use in this study also allowed large knee and hip ranges of motion (RoMs) to be examined. The data-set consisted of 3D kinematic skin marker trajectories of 55 bone and soft tissue markers, mainly attached to the lower limb (List et al. 2013; no spine) captured using an opto-electronic infrared system (100 Hz, Vicon, OMG, Oxford, UK) together with ground reaction force data (2 kHz, Kistler AG, Winterthur, CH) (Figure 1). This data was used to generate the reference movement data (RMD) as well as to scale the models and run the simulation (Modelling approach) with OpenSim as described below.

Reference movement data

While the approaches for kinematic and kinetic assessment vary considerably between motion laboratories, the

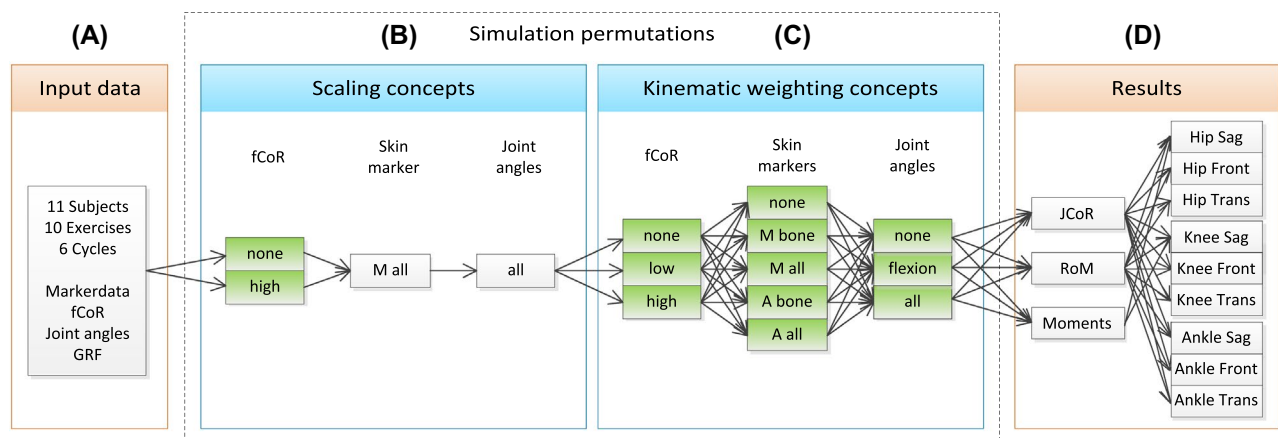


Figure 1. Study design. (A) Kinematic data from skin markers and *fCoRs*, as well as pre-calculated joint angles from the RMD and ground reaction forces, were used as input data. (B) Scaling concepts (green) leading to 2 permutations were used to register the reference model. (C) kinematic weighting concepts ($3 \times 5 \times 3 = 45$ permutations; green) were investigated for driving the scaled musculoskeletal model. (D) To assess simulation robustness, the 3D location of the *fCoRs*, the RoM of the joint angles, as well as maximal external joint moments were calculated and used as evaluation parameters. High: high weighting; low: low weighting; none: no weighting; M all: manually weighted inclusion of all markers; all: weighting of all joint angles in all planes; M bone: manually weighted inclusion of markers based on bone landmarks; A bone: automatic weighted inclusion of markers based on bone landmarks; A all: automatic weighted inclusion of all markers; flexion: weighting of joint angles in the sagittal plane; Sag: sagittal plane; Front: frontal plane; Trans: transverse plane.

approach according to List and co-workers (2013) was used for functionally determining the lower limb joint centre of rotations (*fCoRs*) and functionally defined axis of rotation (*fAoR*) in the knee, acquired during a range of basic motion tasks. The basic motion tasks consist of one reference measurement assessed in the natural standing position of the subject as well as eight different standardised movements (two for each ankle, one for each knee, and one for each hip joint) in order to provide movement data of the segments over a large RoM for each joint. A predefined centre or axis of rotation was then iteratively optimised using the relative movement of the distal to the proximal segment, in order to determine the corresponding *fCoR* or *fAoR*, respectively (List et al. 2013). Joint angles were calculated using a direct kinematics procedure after which external joint moments for each of the 660 cycles were calculated using quasi-static inverse dynamics (List et al. 2013). The resulting subject-specific kinematic data, from here on named the 'RMD' was used to compare results estimated in this study.

Modelling approach

Scaled generic MS models (Delp et al. 2007) were constructed to assess the resultant joint kinetics and kinematics in the ankles, knees and hips of each subject. Here, the 'Gait2392_simbody' model (Yamaguchi & Zajac 1989; Delp et al. 1990; Anderson & Pandy 1999, 2001) was adapted to include 14 body segments and one segment describing the barbell (Figure 2). The reference model therefore comprised 30 degrees of freedom (DoF), including 3 DoFs in each knee and ankle joint, as well as a predefined flexion dependent path of the centre of rotation (CoR) at the knee introduced by Yamaguchi and Zajac (1989). Forty seven skin markers were attached to the reference MS model at segment locations according to List and co-workers (2013) (six markers attached on the elbow and wrist were not included in the MS model) and two on the barbell. Twenty one markers were palpated on bone landmarks, where 25 markers were additionally placed on lower limb segments and subsequently handled as soft tissue markers (Figure 2). Furthermore, six virtual markers were also included in the model at the CoR of the hip, knee and ankle joints. These virtual markers allowed to take the subject specific joint centre positions and movements into account. The chosen coordinate systems and joint angle definitions were consistent with ISB recommendations (Wu & Cavanagh 1995) based on Grood and Suntay (1983).

Subject specific scaling concepts

Two different scaling concepts were used to register the reference MS model: The first scaling concept was based

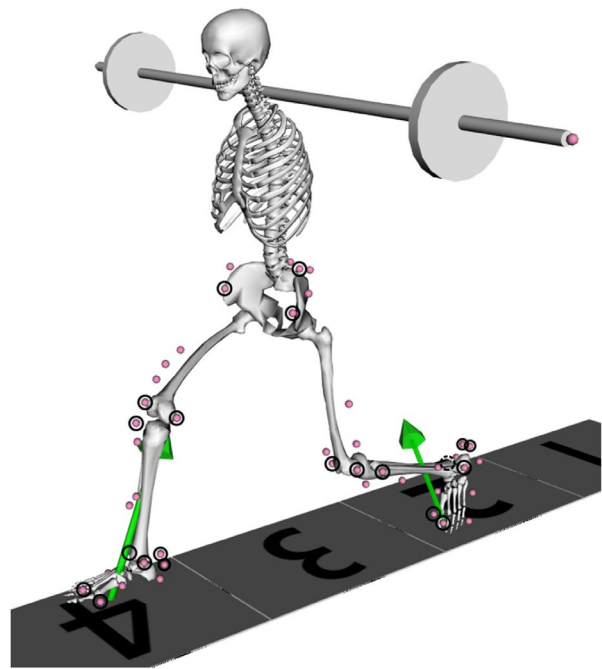


Figure 2. The adapted 'Gait2392_simbody' model with 14 body and one barbell segment resulted in 30 degrees of freedom. 21 markers were palpated on bone landmarks (highlighted with a black circle), while the remaining 25 markers were classified as soft tissue markers. In addition, 6 virtual markers were included at the CoR of the hip, knee and ankle joints.

on the standard operational procedures used in OpenSim (Delp et al. 2007). Here, the segment dimensions were determined according to the bone landmarks. The markers of the reference model were then fitted to the captured marker cloud during an upright standing trial (Figure 1(B)), that included a marker weighting of 5–1 for the palpated bone to soft tissue markers respectively (Figure 2), as well as the pre-calculated joint angles with a weighting of 0.02.

In the second scaling concept, the segment dimensions were based on the distances between the *fCoRs* of the hip, knee and ankle of the RMD of each subject. Keeping the same marker weightings as in the first scaling concept, the *fCoRs* were additionally weighted with a factor of 60 (Figure 1(B)). For determination of the local coordinate system at the knee, the *fAoR* of the knee of the RMD was included in the scaled model.

Kinematic approach

For each subject ($n = 11$) and each scaling concept ($n = 2$), segment kinematics were calculated using the inverse kinematics procedure in OpenSim after which an inverse dynamics analysis was performed to calculate the external joint moments. In order to explore the effects of different standard weighting options available within OpenSim (Delp

et al. 2007), 45 ‘kinematic weighting concepts’ were investigated for driving the inverse kinematics solution. These differed based on skin marker weightings, the in- or exclusion of *fCoRs*, and the in- or exclusion of pre-calculated joint angles (List et al. 2013; Schütz et al. 2014; Figure 1(C)). The skin markers were either neglected completely (weight being 0, Figure 1(C)), or assigned weightings according to four different approaches: (I) only the bone markers (Figure 2) were included and weighted manually with a factor of 1; (II) all markers were weighted manually with a factor of 1; (III) only the bone markers were included, and weighted automatically based on soft tissue artefacts (STA), and (IV) all markers were included, and weighted automatically based on STA. The STA automated weighting procedure was adapted from Heller et al. (2011) and Kratzenstein et al. (2012) using the relative variance of distance between each skin marker and the corresponding segment centre of mass. In order that each segment was considered with equal importance, the sum of all skin marker weighting factors was defined to be 10 on each segment, independent of the number of markers attached to that segment. The *fCoRs* were included as additional virtual markers and either neglected (weighted with 0, Figure 1(C)); weighted low (for the hip (10), knee (10) and ankle (6) joints), or weighted high (100, 100 and 60 respectively) in order to simulate almost complete dependence upon the joint centres alone. Similarly, the absolute joint angles of the pelvis and the relative joint angles between the lumbar, pelvis, thigh and tibia segments using the direct kinematics approach were either neglected, weighted only in the sagittal plane (weighting 0.02), or weighted in all planes (30 DoF; weighting 0.02).

This resulted in 90 possible scaling and kinematic permutations for each of the 6 repetitions of 10 exercises in each of the 11 subjects; and therefore a total of 59,400 individual MS simulations.

Robustness

The trajectories of the joint centres and angles from the inverse kinematics, as well as the external joint moments were compared against the RMD for all 90 scaling and kinematic permutations. To assess the effect on the kinematics, two parameters were evaluated. Firstly, differences in the 3D locations (global coordinate system) of the hip, knee and ankle joints (Δd^{joint}) between the MS simulations (MSs) and the RMD were calculated for each cycle:

$$\Delta d^{joint} = \frac{\sum_{i=1}^n \left| \vec{r}_{MS_i}^{joint} - \vec{r}_{RMD}^{joint} \right|}{n} \quad (1)$$

where \vec{r} is the 3D location of the *joint* (hip, knee and ankle of front and rear limbs), and n is the number of frames in the respective cycle.

Secondly, in a similar manner, the differences in the range of motions (RoMs) ($\Delta RoM^{joint,p}$) of the individual degrees of freedom (p : sagittal [flexion], frontal [adduction] and transversal [rotation]; according to Grood and Suntay (1983)) of each *joint* (hip, knee and ankle) of the front and rear limbs were calculated over each cycle as follows:

$$\Delta RoM^{joint,p} = \left| RoM_{MSs}^{joint,p} - RoM_{RMD}^{joint,p} \right| \quad (2)$$

Additionally, the normalised differences $\Delta RoM_{norm}^{joint,p}$ were computed by dividing $\Delta RoM^{joint,p}$ by $RoM_{RMD}^{joint,p}$ to allow a fair comparison between the different movement types.

As a kinetic evaluation parameter, reported for the hip and knee *joints* only (ankle joint is of low interest during this type of strength exercise and is less affected due to the low external moment), the absolute difference in the maximum external joint moment in the sagittal plane, divided by each subject’s bodyweight, was calculated as follows:

$$\Delta M_{max}^{joint} = \left| M_{MS_{max}}^{joint} - M_{RMD_{max}}^{joint} \right| \quad (3)$$

The mean differences, their standard deviations (SDs), as well as the root-mean-square error (RMSE) were calculated for all 90 permutations for each parameter. To quantify the robustness of each of the scaling and kinematic options (highlighted in green in Figure 1), the RMSEs of the three aforementioned evaluation parameters were averaged and the SDs were calculated for all possible permutations that include that specific option. To provide a fair comparison, each RMSE was normalised (*Norm RMSE*) by dividing the RMSE by its averaged RMSE from all permutations.

Ranking

In order to assess the relative performance of each of the 90 different simulation permutations in a fair manner, a ranking based on each parameter’s *Norm RMSE* was produced. The sum of the three normalised RMSEs (Δd^{joint} , $\Delta RoM^{joint,p}$ and ΔM_{max}^{joint}) was calculated (*sum Norm RMSE*) and ranked according to the values, where a lower *sum Norm RMSE* resulted in a higher ranking, indicating that the kinematics and kinetics of the resulting MS simulation better reflected those of the RMD.

Results

All scaling and kinematic weighting concepts could be successfully simulated in OpenSim except for the six permutations that involved no marker weighting and no *fCoR* weighting. These permutations were therefore not taken into account for further analysis.

Table 1. Averaged RMSEs resulting from the scaling and weighting permutations, including the corresponding SDs. The different columns distinguish the three evaluation parameters: the 3D location of the joint centres (Δd^{Joint}), the RoMs (ΔRoM^{Joint}) and maximal external joint moments (ΔM_{max}^{Joint}). Each of these columns is separated by the two scaling permutations. The first row (All) shows the averaged difference (between the reference and simulated data) of all kinematic weighting permutations, while the following rows show grouped mean values according to the kinematic weighting concepts used.

			Scaling concepts					
			RMSE Δd^{Joint} [mm]		RMSE ΔRoM^{Joint} [°]		RMSE ΔM_{max}^{Joint} [Nm/BW]	
			high	none	high	none	high	none
Kinematic weighting concepts	All		8.5 ± 2.6	18.0 ± 2.9	4.8 ± 7.6	4.5 ± 6.3	0.11 ± 0.14	0.11 ± 0.11
	fCoR	none	11.4 ± 1.0	21.8 ± 1.1	2.1 ± 1.2	2.4 ± 1.4	0.09 ± 0.01	0.11 ± 0.01
		low	7.7 ± 2.0	17.2 ± 1.8	5.2 ± 8.9	4.4 ± 7.0	0.12 ± 0.17	0.11 ± 0.14
		high	6.9 ± 2.2	15.8 ± 1.6	6.7 ± 8.9	6.4 ± 7.6	0.12 ± 0.16	0.11 ± 0.13
	Markers	none	6.2 ± 3.1	15.9 ± 1.5	18.0 ± 13.8	12.9 ± 12.2	0.33 ± 0.29	0.23 ± 0.25
		M bone	9.1 ± 3.1	18.2 ± 3.3	4.0 ± 4.1	4.8 ± 5.8	0.09 ± 0.03	0.11 ± 0.09
		M all	8.5 ± 2.2	18.0 ± 2.9	2.1 ± 1.7	2.5 ± 2.1	0.07 ± 0.01	0.07 ± 0.02
		A bone	8.9 ± 2.3	18.9 ± 3.2	2.3 ± 1.7	2.9 ± 2.1	0.08 ± 0.01	0.09 ± 0.02
	Angles	A all	8.9 ± 2.2	18.4 ± 2.9	2.1 ± 1.4	2.5 ± 1.8	0.07 ± 0.01	0.08 ± 0.02
		none	7.0 ± 3.3	16.6 ± 2.8	6.5 ± 8.4	7.6 ± 9.3	0.16 ± 0.22	0.16 ± 0.18
		flex	8.1 ± 1.8	17.7 ± 2.8	7.6 ± 9.0	5.6 ± 3.1	0.10 ± 0.06	0.09 ± 0.02
		all	10.3 ± 1.1	19.8 ± 2.3	0.4 ± 0.1	0.5 ± 0.1	0.07 ± 0.01	0.08 ± 0.02

Robustness

The scaling concept that included *fCoRs* resulted in smaller RMSEs in Δd^{Joint} than without (Table 1). Similarly, the inclusion of highly weighted *fCoRs* in the kinematic weighting concepts, and omitting other input data (i.e. markers: none, angles: none), resulted in the smallest RMSEs in Δd^{Joint} . Regarding RMSEs of ΔRoM^{Joint} , the inclusion of all precalculated angles in the simulations showed similar RoMs to the RMD and was at least five times smaller than when the pre-calculated angles were excluded. Moreover, this concept subgroup had the smallest SD (0.1°) suggesting one of the most robust combinations. On the other hand, neglecting all skin markers as kinematic input data resulted in large RMSEs for ΔRoM^{Joint} as well as for ΔM_{max}^{Joint} . Furthermore, neglecting pre-calculated joint angles resulted in large RMSEs in ΔM_{max}^{Joint} . In- or exclusion of all other parameters did not seem to play a key role for the evaluation parameters. Compared to the mean RMSEs of ΔM_{max}^{Joint} , large SDs were observed in the permutations where *fCoRs* were included, but also where markers or joint angles were excluded as kinematic input data.

Joint Centres

Looking more specifically at the different joints, a large variation in the difference of 3D locations of the hip, knee and ankle joints (Δd^{Joint}) was observed (Figure 3). However, the average Δd^{Joint} was similar for each the front and the rear limbs in all joints. The mean RMSE for the hip, knee and ankle joints between the MS simulation and RMD was about 136 mm (SD (43 mm)).

Range of motions

The means of the minimal differences in the range of motion in each joint ($\Delta RoM^{Joint,p}$) were below 0.5° in all

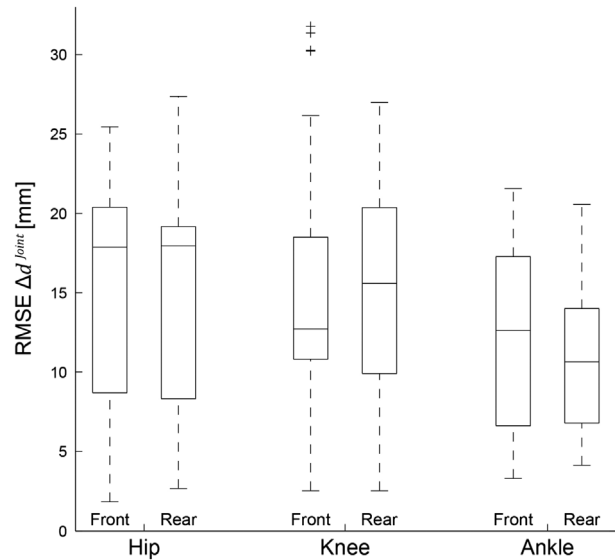


Figure 3. Boxplot of the RMSE of the differences in the 3D locations of the hip, knee and ankle joints ($RMSE \Delta d^{Joint}$) of the front and rear leg between the RMD and simulated locations for all 90 permutations.

joints and all planes, except for adduction and rotation of the rear hip and rotation of the front hip. However, more unstable permutations resulted in unrealistic angles with extreme maximum errors of up to 98° (Table 2). Similar to Δd^{Joint} , comparable errors were found between the joints of the front and trailing limbs. The SDs in all joints and all planes were almost as high as the mean values themselves (Table 2), indicating large differences between the smallest and highest values compared to the RMD.

Moments

The mean as well as the maximum ΔM_{max}^{Joint} were higher in the knee than in the hip (Figure 4). RMSEs of between

Table 2. The mean values of all 90 permutations, its SD, and the RMSE of the differences in the RoMs of the hip, knee and ankle joints in each anatomical plane ($\Delta RoM^{joint,p}$), as well as the normed differences ($\Delta RoM_{norm}^{joint,p}$), are given for the front (above) and rear (below) limbs. Out of all 90 permutations, the maximal values are shown separately for all joints and planes. (flex: flexion, add: adduction, rot: rotation, inv: inversion).

			$\Delta RoM^{joint,p} [^\circ]$				$\Delta RoM_{norm}^{joint,p}$			
			Mean	Max	SD	RMSE	Mean	Max	SD	RMSE
Front	Hip	flex	1.0	5.0	0.8	1.3	0.02	0.11	0.02	0.03
		add	0.8	1.5	0.7	1.1	0.11	0.22	0.11	0.16
		rot	8.5	66.1	7.3	11.2	1.12	9.06	1.23	1.67
	Knee	flex	3.6	53.0	2.5	4.6	0.05	0.66	0.03	0.06
		add	11.3	79.4	7.3	13.7	2.98	19.62	2.65	4.04
		rot	9.6	98.4	10.4	14.4	1.50	14.15	2.01	2.53
	Ankle	flex	2.9	32.7	1.3	3.2	0.10	1.00	0.04	0.11
		rot	4.2	29.3	3.0	5.2	0.75	5.15	0.62	1.00
		inv	3.5	9.5	2.3	4.3	0.44	1.25	0.31	0.56
Rear	Hip	flex	0.9	4.9	0.7	1.1	0.06	0.31	0.06	0.08
		add	1.1	3.5	0.9	1.4	0.12	0.38	0.11	0.16
		rot	5.6	51.3	4.6	7.2	0.78	7.64	0.79	1.12
	Knee	flex	3.2	49.9	2.3	4.0	0.05	0.71	0.03	0.06
		add	7.6	72.4	5.2	9.3	2.80	27.39	2.49	3.77
		rot	6.9	82.1	8.5	11.1	1.37	15.32	1.92	2.38
	Ankle	flex	1.4	16.6	1.3	1.9	0.09	1.00	0.05	0.11
		rot	2.3	10.5	2.2	3.3	0.50	2.42	0.46	0.71
		inv	2.4	7.7	2.1	3.2	0.33	1.00	0.25	0.44

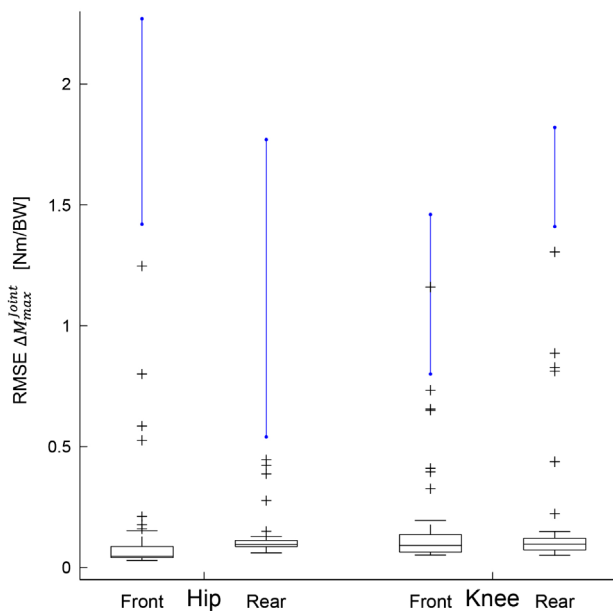


Figure 4. Boxplot of the RMSE of the absolute difference (between the reference and simulated data) in the maximum external joint moment in the sagittal plane, normalised to each subject's bodyweight ($RMSE \Delta M_{max}^{joint}$) for all 90 permutations in the hip and knee joints of the front and rear limbs. For comparison, the blue lines report the ranges of absolute external moments over all 10 types of split squats analysed by Schütz and co-workers (2014), and demonstrate that in certain cases, the error is as large as the measured values.

approximately 0.05 and 0.1 Nm/BW were observed across all four joints, thus representing 3–9% of the absolute joint moments. Similar to the RoM, more unstable permutations resulted in unrealistic joint loading conditions with extreme maximum errors up to 1.3 Nm/BW.

Ranking

The concepts leading to the highest 20 rankings and that therefore best fit the RMD all used the scaling concept with the inclusion of *fCoRs* (Table 3). In addition, the highest 17 rankings included *fCoRs* in the inverse kinematics procedure, where the first 9 (except the permutation ranked 4) all used a high weighting. The inclusion or exclusion of the skin markers seemed to make little or no difference to the total error. Furthermore, the concepts leading to the first 6 rankings all used the inclusion of pre-calculated angles in all planes. Importantly the rankings 7–9 all excluded (none) the use of joint angles, but were otherwise the same permutations as 3, 5 & 6 regarding the scaling concepts and the inclusion of *fCoR* and skin marker weightings. These permutations (rank 7–9) produced similar levels of total error (*Sum Norm RMSE* between 1.36 and 1.39) compared to the permutations ranked 1–6; however, the errors (*Norm RMSEs*) of each parameter (Δd^{joint} , ΔRoM^{joint} , and ΔM_{max}^{joint}) were distributed differently compared to the errors seen for ranks 1–6. In fact, this trend was also more generally observed where Δd^{joint} and ΔRoM^{joint} both displayed a clear dependency on the usage of joint angles. Here, Δd^{joint} was larger in permutations that included joint angles, while ΔRoM^{joint} was lower, and vice versa.

Discussion

With musculoskeletal modelling simulations becoming increasingly available, access to an individual's internal loading conditions now opens perspectives for improvements in subject specific training, rehabilitation regimes

Table 3. Rankings were assigned to each permutation based on the parameters' normed RMSEs (*Norm RMSE*). Each parameter was ranked according to the total error i.e. the difference in 3D location of the joint centres of rotations, angles and moments (*sum norm RMSE*), where a lower *sum norm RMSE* resulted in a higher ranking, indicating that the MS simulation was closer to the reference motion data.

Ranking	Scaling concept		Kinematic weighting concept		Norm RMSE			Sum norm RMSE
	<i>fCoR</i>	<i>fCoR</i>	Skin markers	Joint angles	Δd^{joint} [mm]	$\Delta RoM^{joint,p}$ [mm]	ΔM^{joint}_{max} [mm]	
1	high	high	none	all	0.73	0.06	0.55	1.34
2	high	high	M bone	all	0.72	0.06	0.56	1.34
3	high	high	M all	all	0.72	0.06	0.57	1.35
4	high	low	none	all	0.74	0.06	0.55	1.35
5	high	high	A all	all	0.71	0.06	0.58	1.35
6	high	high	A bone	all	0.71	0.06	0.58	1.36
7	high	high	M all	none	0.38	0.46	0.54	1.37
8	high	high	A all	none	0.38	0.46	0.54	1.38
9	high	high	A bone	none	0.38	0.47	0.53	1.39
10	high	low	M bone	all	0.72	0.07	0.61	1.40
11	high	low	M all	all	0.73	0.07	0.62	1.42
12	high	low	M bone	none	0.44	0.44	0.56	1.43
13	high	low	M all	none	0.47	0.41	0.56	1.44
14	high	low	A all	all	0.76	0.07	0.66	1.50
15	high	low	A bone	all	0.77	0.08	0.68	1.52
16	high	low	A all	none	0.53	0.44	0.61	1.59
17	high	low	A bone	none	0.54	0.44	0.62	1.60
18	high	none	M all	all	0.86	0.08	0.72	1.66
19	high	none	A all	all	0.88	0.08	0.74	1.70
20	high	none	A bone	all	0.89	0.08	0.76	1.74
...
81	none	high	none	none	1.12	5.05	4.58	10.74
82	high	high	none	none	0.21	5.00	6.15	11.36
83	high	low	none	none	0.21	5.14	6.33	11.68
84	none	low	none	none	1.14	5.22	5.45	11.81
85	high	none	none	all	No numerical solution achieved			
86	high	none	none	flex				
87	high	none	none	none				
88	none	none	none	all				
89	none	none	none	flex				
90	none	none	none	none				

and even targeted therapies. However, with a variety of potential errors for relating the observed motion capture to the scaled generic MS model in an inverse kinematics approach, it remains unclear how best to achieve robust MS modelling analyses in terms of producing minimal errors between kinematics calculated using direct and inverse kinematics procedures. As such, we aimed to determine the parameters that allow scaled generic musculoskeletal models to be registered to the recorded motion data in the most robust manner possible, but also understand the levels of error involved. Here, open source musculoskeletal simulation software (OpenSim SimTk; Delp et al. 2007) was used to explore the effects of 90 different permutations of scaling and kinematic weighting concepts on the robustness of the resulting MS analyses.

Our results indicate an overall difference (mean of 45 permutations) in the 3D locations of the hip, knee and ankle joints (Δd^{joint}) throughout complete activity cycles (in this case squats) of 8.5 mm when functionally derived joint centres were included in the scaling process, whereas mean registration errors up to 18.0 mm were observed with their exclusion (Table 1). These results are comparable to values reported in the literature varying between 8

and 16 mm (Leardini et al. 1999; Hicks & Richards 2005; Cereatti et al. 2009; Sangeux et al. 2011) for approaches that also included functional joint centres, and up to 38 mm (Bell et al. 1990) for those that did not. Similarly, in the estimation of joint centres, errors of 19–36 mm have been observed using anthropometrical data (Bell et al. 1990), suggesting that the source of different errors is consistent with our analyses using permutations without the inclusion of *fCoRs*.

Joint centres

Despite the very different kinematics of the lower limbs during the split squat activities, the average Δd^{joint} was similar for each joint. The lowest single RMSE of Δd^{joint} of all permutations was 1.8 mm, and was found in the hip joint of the front leg (Figure 3), values that were comparable to the errors reported in other studies, including Heller and co-workers (2011), whose weighted optimal common shape technique achieved hip joint centres with a precision of 3.4 ± 1.1 mm. The lowest average errors over all permutations observed for a joint, however, were 10.9 mm, found in the ankle joint of the rear leg – an error

value that could be considered representative of general or standard procedures that aim to reproduce measured kinematics in MS models. Since the CoR of the ankle joint has only low displacement in space, as well as the lowest soft tissue coverage compared to the hip and the knee (Barré et al. 2015; Camomilla et al. 2015; Thouzé et al. 2016), it is entirely reasonable that this joint experiences the lowest STA and therefore exhibited the lowest mean differences to the RMD. However, based on the presented rankings, targeted weighting and scaling of measurement input during scaling and inverse kinematics can reduce considerably the errors down to a few millimetres, or up to a factor of 8 compared to their mean RMSE values (hip of front limb).

Range of motions

Large RMSEs and SDs compared to the mean $\Delta RoM^{Joint,p}$ (Table 2) indicate only low levels of robustness in this parameter. Here, since mean and RMSE outliers of up to 98° were found, most likely due to non-physiological or unnatural simulation postures resulting from under-determined boundary conditions, it is important to avoid unrealistic segment ‘flipping’, and ensure appropriate RoMs for each joint within each anatomical plane. Importantly, permutations that excluded the use of skin markers and joint angles resulted in unrealistic solutions (rankings 81–84, Table 3), while permutations that excluded $fCoRs$ and skin markers were even worse, where upon no numerical solution could be achieved (rankings 85–90). In studies investigating the effects of STA on real segment kinematics using photogrammetric and fluoroscopic approaches, comparable errors of up to 192 and 117% were found in the RoM for knee abduction–adduction and internal–external rotation respectively (Stagni et al. 2005). Similarly, the observed RMSEs for flex/ext: 7.3–47.3%; int/ext: 46.7–102.3%; abd/add: 29.3–93.5% for open-chain knee flexion, hip axial rotation, level walking, and step-up exercises suggest that such errors are not only joint, but also activity dependent (Akbarshahi et al. 2010; c.f. Table 2). However, the lowest $\Delta RoM^{Joint,p}$ of all 90 permutations in our study were below 0.5° in all planes, indicating a good representation of the RMD, hence signifying that robust solutions can be achieved when permutations including pre-calculated angles in all planes were employed.

Moments

An average RMSE of 0.11 Nm/BW was computed for the external joint moment (ΔM_{max}^{Joint}) across all permutations. This value is within the observed range of mean error of external joint moments (sagittal plane; hip: –0.05–0.15

Nm/kg and knee: 0.04 Nm/kg) (Kirkwood et al. 1999; Besier et al. 2003) calculated using different approaches during gait, despite the fact that the magnitudes of the moments in this study were considerably higher. Here, large SDs were observed across the results for different permutations (Figure 4), indicating that scaling and kinematic weighting concepts could lead to a considerable variability in the levels of robustness of the calculated joint moments. Compared to RoM and CoRs, the parameter ΔM_{max}^{Joint} seems to be robust over many permutations, hence suggesting low sensitivity of this parameter to any specific input, as long marker and angle weighting are included; however, non-physiological kinematic simulation clearly affects the moments and any resulting MS analysis, and should be avoided at all costs.

General

Interestingly, the RMSEs of ΔRoM^{Joint} and ΔM_{max}^{Joint} differ considerably with the inclusion or exclusion of weighting factors for the pre-calculated joint angles in the MS simulation (Table 1), even although the applied weighting factors were extremely small (0.02). Since SDs of the RMSEs of ΔRoM^{Joint} and ΔM_{max}^{Joint} were in general large when pre-calculated joint angles or all skin markers were excluded from the kinematic weighting (Table 1), the accuracy of reproducing the RMD remains somewhat unknown. On the other hand, by including pre-calculated joint angles, low RMSEs as well as low SDs can be achieved for all three parameters (hence indicating high robustness). Since the outcomes of a MS simulation are highly dependent on the ability to accurately reproduce the RMD, and therefore reliant upon the scaling and kinematic weighting concepts, the final permutation chosen should be directly based on the specific aim of the study, e.g. if accurate determination of movements of a specific joint is required or kinematic or kinetic aspects are of high interest.

To consider all these aspects, a specific ranking was developed to evaluate the different weighting concepts that could then be used for future studies (Table 3). In our case, all permutations of the first 17 rankings included $fCoRs$ in both the scaling and the kinematic weighting concepts. Therefore, the inclusion of $fCoRs$ in the scaling procedure in the simulation, instead of simply using anthropometric based data, is appropriate. Permutations that only used skin marker data to scale the reference MS model and register the kinematic movement without the inclusion of $fCoRs$ led to a rank above 55 and resulted in a *Sum rel RMSE* of 2.75 (*Norm RMSE*: $\Delta d^{Joint} = 1.70$; $\Delta RoM^{Joint} = 0.09$; $\Delta M_{max}^{Joint} = 0.96$) or higher. Due to efficiency reasons or if pre-calculated joint angles are not available, rank 7 with a *Sum rel RMSE* of 1.37 should be used such that low errors can be achieved. Despite being

ranked only 5, the solution including *fCoRs*, with automatic weighting of the skin markers based on STA and joint angles clearly also has positive attributes: firstly, the *Sum rel RMSE* is almost as low as the rankings above it. Secondly, by including all weighting possibilities, large errors can be avoided and high levels of robustness can be achieved. Most importantly, however, the automated skin marker weighting process is the most objective approach for weighting skin markers in a batch simulation process. Due to these positive attributes, this scaling and kinematic weighting concept is therefore recommended as a general approach to ensure that musculoskeletal simulation results are both objective and robust.

Two main limitations of this study should be mentioned: The chosen model was developed for gait analyses and might be inaccurate when analysing motions with high degrees of knee flexion (such as the split squats simulated in this study). This limitation has also been noted by the authors of this particular OpenSim model (OpenSim-Documentation 2015), and is a general problem in MS modelling. As far as we are aware, there is no existing and validated model, either in OpenSim or in another musculoskeletal simulation software that is able to satisfy all these conditions. The second limitation was the lack of true gold standard evaluation data such as dual-plane fluoroscopic data combined with instrumented joint implants. Furthermore, the evaluation parameters $\Delta RoM^{joint,p}$ and Δd^{joint} are directly linked to the pre-calculated joint angles of the RMD and the 3D location of the *fCoRs*. Since the calculated RMD might be affected by prediction errors itself, another set of data might lead to different prediction errors and thus to different evaluation result. In order to minimise the influence of this limitation, the robustness was calculated based on RMSEs and not absolute differences. Here, robustness based on RMSEs will reduce the influence of different subject-specific data since this value is mainly based on the differences between the scaling and kinematic weighting concepts and not only on the RMD itself.

Since current results are specific to the analyses implemented in OpenSim, transferability to other musculoskeletal software packages is not guaranteed. While the presented concepts and guidelines might be adapted manually for use in other musculoskeletal simulation software packages, the results, suggestions, and guidelines were primarily targeted for general use in OpenSim, and will therefore be most straight-forward for implementation there.

This study provides a guideline for scaling and weighting concepts of input data for the inverse kinematics procedure in MS simulations. Furthermore, the typical errors involved in using scaling and kinematic weighting concepts are presented. The results indicate that the scaling and weighting of RMD that includes *fCoRs*, pre-calculated

joint angles, and skin markers, provides a sound basis for ensuring robust and high quality scaling of the reference MS models and consequent registration of kinematic data for the individualisation of MS models.

Disclosure statement

No potential conflict of interest was reported by the authors.

References

- Akbarshahi M, Schache AG, Fernandez JW, Baker R, Banks S, Pandy MG. 2010. Non-invasive assessment of soft-tissue artifact and its effect on knee joint kinematics during functional activity. *J Biomech.* 43:1292–1301.
- Anderson FC, Pandy MG. 1999. A dynamic optimization solution for vertical jumping in three dimensions. *Comput Methods Biomech Biomed Eng.* 2:201–231.
- Anderson FC, Pandy MG. 2001. Dynamic optimization of human walking. *J Biomech Eng.* 123:381–390.
- Arnold EM, Ward SR, Lieber RL, Delp SL. 2010. A model of the lower limb for analysis of human movement. *Ann Biomed Eng.* 38:269–279.
- Banks S, Hodge WA. 1996. Accurate measurement of three-dimensional knee replacement kinematics using single-plane fluoroscopy. *IEEE Trans Biomed Eng.* 43:638–649.
- Barré A, Jolles BM, Theumann N, Aminian K. 2015. Soft tissue artifact distribution on lower limbs during treadmill gait: influence of skin markers' location on cluster design. *J Biomech.* 48:1965–1971.
- Bell AL, Pedersen DR, Brand RA. 1990. A comparison of the accuracy of several hip center location prediction methods. *J Biomech.* 23:617–621.
- Besier TF, Sturmeiers DL, Alderson JA, Lloyd DG. 2003. Repeatability of gait data using a functional hip joint centre and a mean helical knee axis. *J Biomech.* 36:1159–1168.
- Blajer W, Czaplicki A, Dziewiecki K, Mazur Z. 2010. Influence of selected modeling and computational issues on muscle force estimates. *Multibody Syst Dyn.* 24:473–492.
- Bobbert MF. 2001. Dependence of human squat jump performance on the series elastic compliance of the triceps surae: a simulation study. *J Exp Biol.* 204:533–542.
- Camomilla V, Bonci T, Dumas R, Chèze L, Cappozzo A. 2015. A model of the soft tissue artefact rigid component. *J Biomech.* 48:1752–1759.
- Cereatti A, Donati M, Camomilla V, Margheritini F, Cappozzo A. 2009. Hip joint centre location: an ex vivo study. *J Biomech.* 42:818–823.
- Charlton I, Tate P, Smyth P, Roren L. 2004. Repeatability of an optimised lower body model. *Gait Posture.* 20:213–221.
- Correa TA, Pandy MG. 2011. A mass-length scaling law for modeling muscle strength in the lower limb. *J Biomech.* 44:2782–2789.
- De Groot F, Van Campen A, Jonkers I, De Schutter J. 2010. Sensitivity of dynamic simulations of gait and dynamometer experiments to hill muscle model parameters of knee flexors and extensors. *J Biomech.* 43:1876–1883.
- Delp SL, Loan JP, Hoy MG, Zajac FE, Topp EL, Rosen JM. 1990. An interactive graphics-based model of the lower extremity to study orthopaedic surgical procedures. *IEEE Trans Biomed Eng.* 37:757–767.

- Delp SL, Anderson FC, Arnold AS, Loan P, Habib A, John CT, Guendelman E, Thelen DG. 2007. OpenSim: open-source software to create and analyze dynamic simulations of movement. *IEEE Trans Biomed Eng.* 54:1940–1950.
- Ehrig RM, Taylor WR, Duda GN, Heller MO. 2006. A survey of formal methods for determining the centre of rotation of ball joints. *J Biomech.* 39:2798–2809.
- Ehrig RM, Taylor WR, Duda GN, Heller MO. 2007. A survey of formal methods for determining functional joint axes. *J Biomech.* 40:2150–2157.
- Graham J. 2002. Barbell Lunge. *Strength Cond J.* 24:30–32.
- Grood ES, Suntay WJ. 1983. A joint coordinate system for the clinical description of three-dimensional motions: application to the knee. *J Biomech Eng.* 105:136–144.
- Heller MO, Kratzstein S, Ehrig RM, Wassilew G, Duda GN, Taylor WR. 2011. The weighted optimal common shape technique improves identification of the hip joint center of rotation *in vivo*. *J Orthop Res.* 29:1470–1475.
- Hicks JL, Richards JG. 2005. Clinical applicability of using spherical fitting to find hip joint centers. *Gait Posture.* 22:138–145.
- Ito M, Akima H, Fukunaga T. 2000. In vivo moment arm determination using B-mode ultrasonography. *J Biomech.* 33:215–218.
- Jonkers I, Sauwen N, Lenaerts G, Mulier M, Van der Perre G, Jaecques S. 2008. Relation between subject-specific hip joint loading, stress distribution in the proximal femur and bone mineral density changes after total hip replacement. *J Biomech.* 41:3405–3413.
- Kirkwood RN, Culham EG, Costigan P. 1999. Radiographic and non-invasive determination of the hip joint center location: effect on hip joint moments. *Clin Biomech.* 14:227–235.
- Kratzstein S, Kornaropoulos EI, Ehrig RM, Heller MO, Pöppel BM, Taylor WR. 2012. Effective marker placement for functional identification of the centre of rotation at the hip. *Gait Posture.* 36:482–486.
- Leardini A, Cappozzo A, Catani F, Toksvig-Larsen S, Petitto A, Sforza V, Cassanelli G, Giannini S. 1999. Validation of a functional method for the estimation of hip joint centre location. *J Biomech.* 32:99–103.
- Lewis CL, Sahrmann SA, Moran DW. 2009. Effect of position and alteration in synergist muscle force contribution on hip forces when performing hip strengthening exercises. *Clin Biomech.* 24:35–42.
- List R, Foresti M, Gerber H, Goldhahn J, Rippstein P, Stüssi E. 2012. Three-dimensional kinematics of an unconstrained ankle arthroplasty: a preliminary in vivo videofluoroscopic feasibility study. *Foot Ankle Int.* 33:883–892.
- List R, Gerber H, Foresti M, Rippstein P, Goldhahn J. 2012. A functional outcome study comparing total ankle arthroplasty (TAA) subjects with pain to subjects with absent level of pain by means of videofluoroscopy. *Foot Ankle Surg.* 18:270–276.
- List R, Gülay T, Stoop M, Lorenzetti S. 2013. Kinematics of the trunk and the lower extremities during restricted and unrestricted squats. *J Strength Cond Res.* 27:1529–1538.
- Liu MQ, Anderson FC, Pandy MG, Delp SL. 2006. Muscles that support the body also modulate forward progression during walking. *J Biomech.* 39:2623–2630.
- Lu T-W, O'Connor JJ, Taylor SJ, Walker PS. 1997. Validation of a lower limb model with *in vivo* femoral forces telemetered from two subjects. *J Biomech.* 31:63–69.
- Moeslund TB, Hilton A, Krüger V. 2006. A survey of advances in vision-based human motion capture and analysis. *Comput Vis Image Underst.* 104:90–126.
- OpenSim-Documentation. 2015. OpenSim Documentation 3.3: Musculoskeletal Models.
- Pandy MG, Zajac FE, Sim E, Levine WS. 1990. An optimal control model for maximum-height human jumping. *J Biomech.* 23:1185–1198.
- Peters A, Galna B, Sangeux M, Morris M, Baker R. 2010. Quantification of soft tissue artifact in lower limb human motion analysis: a systematic review. *Gait Posture.* 31:1–8.
- Piazza SJ, Delp SL. 2001. Three-dimensional dynamic simulation of total knee replacement motion during a step-up task. *J Biomech Eng.* 123:599–606.
- Sangeux M, Peters A, Baker R. 2011. Hip joint centre localization: evaluation on normal subjects in the context of gait analysis. *Gait Posture.* 34:324–328.
- Schellenberg F, Oberhofer K, Taylor WR, Lorenzetti S, Lorenzetti S. 2015. Review of modelling techniques for in vivo muscle force estimation in the lower extremities during strength training. *Computational Math Methods Med.* 2015:1–12.
- Schütz P, List R, Zemp R, Schellenberg F, Taylor WR, Lorenzetti S. 2014. Joint angles of the ankle, knee, and hip and loading conditions during split squats. *J Appl Biomech.* 30:373–380.
- Shippen JM, May B. 2010. Calculation of muscle loading and joint contact forces during the rock step in Irish dance. *J Dance Med Sci.* 14:11–18.
- van Soest AJ, Schwab AL, Bobbert MF, van Ingen Schenau GJ. 1993. The influence of the biarticularity of the gastrocnemius muscle on vertical-jumping achievement. *J Biomech.* 26:1–8.
- Stagni R, Fantozzi S, Cappello A, Leardini A. 2005. Quantification of soft tissue artefact in motion analysis by combining 3D fluoroscopy and stereophotogrammetry: a study on two subjects. *Clin Biomech.* 20:320–329.
- Taylor WR, Ehrig RM, Duda GN, Schell H, Seebeck P, Heller MO. 2005. On the influence of soft tissue coverage in the determination of bone kinematics using skin markers. *J Orthop Res.* 23:726–734.
- Taylor WR, Kornaropoulos EI, Duda GN, Kratzstein S, Ehrig RM, Arampatzis A, Heller MO. 2010. Repeatability and reproducibility of OSSCA, a functional approach for assessing the kinematics of the lower limb. *Gait Posture.* 32:231–236.
- Thouzé A, Monnet T, Bélaïse C, Lacouture P, Begon M. 2016. A chain kinematic model to assess the movement of lower-limb including wobbling masses. *Comput Methods Biomech Biomed Eng.* 19:707–716.
- Winby CR, Lloyd DG, Kirk TB. 2008. Evaluation of different analytical methods for subject-specific scaling of musculotendon parameters. *J Biomech.* 41:1682–1688.
- Wu G, Cavanagh PR. 1995. ISB recommendations for standardization in the reporting of kinematic data. *J Biomech.* 28:1257–1261.
- Yamaguchi GT, Zajac FE. 1989. A planar model of the knee joint to characterize the knee extensor mechanism. *J Biomech.* 22:1–10.
- Zemp R, List R, Gülay T, Elsig JP, Naxera J, Taylor WR, Lorenzetti S. 2014. Soft tissue artefacts of the human back: comparison of the sagittal curvature of the spine measured using skin markers and an open upright MRI. *PLoS One.* 9:e95426.